

Sonography for Assessment of Elbows in Hemophilic Children: A Systematic Protocol

Frederico Xavier¹, Ningning Zhang⁴, Arun Mohanta², Pamela Hilliard¹, Carina Man², Debra Drossmann², Ann Marie Stain¹, Victor Blanchette¹ and Andrea S Doria^{2,3*}

¹Division of Hematology/Oncology, Research Institute, The Hospital for Sick Children, Toronto, Ontario, Canada

²Department of Diagnostic Imaging and Pediatrics, Research Institute, The Hospital for Sick Children, Toronto, Ontario, Canada

³Department of Medical Imaging, University of Toronto, Toronto, Ontario, Canada

⁴Department of Radiology, Children's Hospital, Beijing, China

Abstract

Evaluation of joints using sensitive non-invasive tools is important for diagnosis and follow-up of hemophilic patients who are continuously at risk of development and/or progression of arthropathy. Because conventional radiography is inadequate for assessing early arthropathic changes in hemophilic patients, there has been an increasing interest in the development of systematic protocols and scoring systems using magnetic resonance imaging (MRI) and ultrasound for evaluating hemophilic arthropathy in recent years. Given some advantages of ultrasound over MRI for this purpose, namely easier access, lower costs and no need for sedation in younger patients, detailed sonographic protocols have recently been proposed for assessment of large joints, most notably knees and ankles, which are most frequently affected by hemophilic arthropathy. Due to the challenges that the elbow joint offers to the reproducibility of positioning of the extremity on ultrasound which is an operator dependent imaging modality, the elbow joint requires dedicated attention. In this paper, we present a systematic protocol for sonographic data acquisition of the elbow in hemophilic children along with examples of findings of joint effusion, synovial hypertrophy, hemosiderin deposition, surface erosions, subchondral cysts and cartilage loss. We also correlate the ultrasound findings with corresponding MR images demonstrating the anatomic planes used for imaging acquisition. The development of a systematic protocol for ultrasound imaging acquisition of elbows in hemophilic children opens avenues for the development/refinement of ultrasound scales for assessment of hemophilic arthropathy which should reduce the opportunity for inter- and intra-operator variability during acquisition of images. Further validation of the proposed systematic protocol for assessment of arthropathic changes in hemophilic elbows is required for its future use in cross-sectional and longitudinal clinical trials. Standardization and validation of such protocols is essential for comparison of results of clinical trials conducted in different hemophilia centres across the world.

Keywords: Hemophilia; Joint disease; Elbows; Pediatric; Scoring system; Ultrasound; Magnetic resonance imaging

Introduction

Recurrent hemarthrosis in hemophiliacs leads to synovial inflammation and proliferation associated with absorption of hemosiderin and red cell products. The breakdown of extravasated blood from synovial vessels ultimately leads to synovitis, cartilage loss and subchondral bone irregularity [1].

The age of onset and frequency of hemarthrosis is most frequently determined by the level of factor deficiency, which can be severe (factor VIII or IX baseline activity $\leq 1\%$), moderate (residual activity 2%-5%) or mild (residual activity $> 5\%$) [2]. However, it typically starts in the first and second decades of life [3,4].

The goal in the therapy of hemophiliacs is the long-term suppression of spontaneous bleeding, or its suppression for a defined interval of time through prophylactic administration of coagulation factors [5]. Nevertheless, small doses of coagulation factors do not totally exclude subclinical bleeds. Recognizing minimal changes in hemophilic joints and treating the patients accordingly is crucial for a favourable functional joint outcome. Assessing the anatomic joint status both at a given timepoint and longitudinally in hemophilic patients with different degrees of severity of arthropathy enables clinicians to adjust treatment doses and re-visit therapeutic strategies. Medical imaging of joints of hemophilic children is valuable in detecting mild, moderate and severe abnormalities, staging their severity, following the effects of treatment and diagnosing prior subclinical bleeds [6,7]. Within the clinically available imaging modalities for assessment of pediatric joints, ultrasound is particularly appealing since it is economic, easily accessible, does not require sedation for young children, does not bear

radiation and is sensitive for detection of soft tissue changes such as effusions and synovial hyperplasia [8].

Approximately 80–90% of bleeding episodes in hemophilia occur in the musculoskeletal system, most notably in large joints (elbows, knees, ankles) [6]. However, few detailed sonographic protocols [9] are currently available for assessment of hemophilic elbows.

The human elbow is constituted of three articulations: humeroulnar, humeroradial and pivot-type synovial joint with articulation between the head of the radius and the radial notch of the ulna [10]. These three articulations allow different degrees of flexion, extension, supination and pronation of the forearm at the elbow which makes the reproducibility of positioning of the extremity on imaging examinations a challenging task, most notably on ultrasound which is operator dependent. In addition, when the elbow is in anatomic position, the long axis of the forearm typically has an offset (lateral inclination or valgus at the elbow) of about 19° from the long axis of the humerus [11] which constitutes an additional component of

***Corresponding author:** Andrea S Doria, The Hospital for Sick Children, Department of Diagnostic Imaging, 555 University Avenue, Toronto, Ontario M5G1X8, Canada, Tel: 416-813-6079; Fax: 416-813-7591; E-mail: andrea.doria@sickkids.ca

Received January 24, 2011; **Accepted** March 04, 2012; **Published** March 12, 2012

Citation: Xavier F, Zhang N, Mohanta A, Hilliard P, Man C, et al. (2012) Sonography for Assessment of Elbows in Hemophilic Children: A Systematic Protocol. *Rheumatol Curr Res* S2:004. doi:10.4172/2161-1149.S2-004

Copyright: © 2012 Xavier F, et al. This is an open-access article distributed under the terms of the Creative Commons Attribution License, which permits unrestricted use, distribution, and reproduction in any medium, provided the original author and source are credited.

variability for repeated measurements depending on the position of the joint during scanning. Because of the aforementioned challenges for imaging the elbow joint, the development of imaging protocols for the elbow joint has been deferred to other articulations such as knees and ankles which are easier to assess on imaging. As such, the development of a standardized protocol for elbow joints in hemophilic children needs to be further defined.

The purpose of this study was to develop an ultrasound protocol that could enable visualization of synovial and perisynovial tissue along the elbow bursae, synovial fluid, articular cartilage and adjacent subchondral region within the field-of-field that conventional high resolution ultrasound probes can assess in clinical practice. This paper focuses on a systematic approach for data acquisition of pediatric hemophilic elbows demonstrating the anatomic planes used for this purpose and providing corresponding ultrasound-MR images of soft tissue and osteochondral findings of hemophilic arthropathy in selected elbow joints.

Methods

Patients

This study received approval by our Institutional Ethics Board to be prospectively carried out in our tertiary centre. Informed consent was obtained from all patients' parents and/or patients themselves. A convenience sample of 7 boys with hemophilia A (severe, n=6; moderate, n=1) and 1 boy with von Willebrand disease with ages ranging between 6 and 17 years (median, 10) had their most affected elbow scanned by ultrasound (gray-scale and color Doppler) and MRI and underwent physical examination using the version 2.0 of the Hemophilia Joint Health Score (HJHS) [12] on the same day between June 2009 and December 2011. If the patients already had an x-ray of the study joint done within 6 months from their ultrasound-MRI-physical examinations no further radiographs were obtained for this study. Otherwise, X-rays of the study joint were obtained on the same day of the other examinations. Patients had only the most severely affected elbow joint examined.

Systematic imaging protocol

Technical parameters: To image the elbow joint comprehensively, ultrasound images from different planes in supine (Figure 1, Figure 2 and Figure 3) and prone (Figure 4 and Figure 5) positions were obtained on gray-scale and color Doppler. The images shown in this paper were obtained with a iU22 xMATRIX (Philips Healthcare, Bothell, WA) ultrasound scanner using a L17-5 MHz linear-array transducer and with a 1.5T (MAGNETOM Avanto, Siemens, Erlangen, Germany) MR unit with use of wrapped around the extremity body coils or extremity coils.

The ultrasound protocol included sagittal and axial gray-scale images obtained with depth and gain adjustable to the patient's body habitus and color Doppler images acquired with low filter, 700 Hz of pulse repetition frequency and 80% intensity. The duration of the US examination on this study was approximately 30 minutes per joint.

The MRI protocol employed axial Multi-Echo Data Image Combination [MEDIC]) (TR / TE 450/19 ms; flip angle, 180°; slice thickness/gap, 3/0 mm; FOV, 150 mm; matrix, 256 x 192), sagittal T1 turbo spin-echo (TSE) (TR/TE 568/10 ms; flip angle, 180°; slice thickness/gap, 3/0 mm; FOV, 150 mm; matrix, 256 x 256), sagittal T2 TSE (TR/TE 4200/96 ms; flip angle, 180°; slice thickness/gap, 3/0 mm; FOV, 170 mm; matrix, 256 x 256), sagittal and coronal 3D water excitation Double Echo Steady State [DESS] (TR/TE 27.63/8.76 ms;

slices/slab 80; slice thickness/gap, 1.25/0 mm; FOV, 150 mm; matrix, 256 x 256) and coronal proton density (PD) TSE (TR/TE 3800/42 ms; slice thickness/gap, 3/3.3 mm; FOV, 170 mm; matrix, 320 x 256) sequences. The duration of this MRI protocol for a single elbow joint was approximately 30 minutes.

Ultrasound acquisition technique

The Table summarizes the transducer positions scanned in the sagittal, coronal and axial planes. Standard anatomic descriptions for the level of transducer position were as follows: L1 for the proximal articular surface (above the elbow joint), L2 for the joint space and L3 for the distal articular surface (below the elbow joint) as previously described for knees and ankles [13].

The scanning sequences were obtained in such a way that the anterior scans (obtained in supine position) were performed before proceeding to the posterior scans (obtained in prone position), to avoid multiple changes in patient position. The true lateral and true medial (coronal) planes could have been obtained either in supine or prone position, however for the sake of easiness we have obtained them with the patient lying in supine position in this study. The probe was positioned longitudinally or transversally in relation to the humeral bone axis with the patient in supine or prone position as appropriate with the upper extremity in neutral position (extension).

With regard to color Doppler ultrasound imaging, we defined the planes that best capture the vascularity of perisynovial tissues in the protocol (Table), which lie mainly at the level of the olecranean bursae.

Clinical and radiographic scores of hemophilic elbows

Pettersson x-ray scores [14] ranged between 1 and 8 (median, 4) and study joint HJHS scores, between 2 and 12 (median, 8.5). The number of lifetime study joint prior bleeds ranged between 2 and 20 (median, 6). Informed consent was obtained by the patient's parents/ themselves prior to the aforementioned research examinations.

Ultrasound findings on hemophilic arthropathy of the elbow

The use of ultrasound for diagnosis of arthropathic lesions in hemophilic joints presents: (i) the disadvantage of requiring an expert physician specialized in ultrasound; (ii) the need for scanning time similar to that required for an MRI examination of that specific joint for a detailed sonographic examination (with the advantage of not requiring sedation in young children) and (iii) the advantage of applying a technology that is available at most hospitals/clinics where hemophiliacs are treated which enables the follow-up of hemarthrosis, synovitis or muscle hematoma in the extremities.

Gray-scale ultrasound is able to determine the degree of soft tissue inflammation, detect the presence of intra-articular fluid, synovial hypertrophy and hemosiderin deposition and evaluate the status of the articular cartilage along the periphery of the joint. It is well known that ultrasound allows differentiation between synovitis (synovial thickening) and cartilage involvement and between synovial hypertrophy and joint effusion [15,16]. Ultrasound is also useful in identifying heterotopic calcifications, bursal haemorrhage and inter- or intramuscular haemorrhage. However, ultrasound cannot differentiate intra-articular blood from infected synovial fluid (septic arthritis) as this requires information on clinical and laboratory parameters [6].

Figure 6 and Figure 7 illustrate specific findings of hemophilic arthropathy of the elbow on ultrasound and MRI which include soft tissue [joint effusion (Figure 6), synovial hypertrophy and hemosiderin deposition (Figure 6 and Figure 7)] and osteochondral tissue

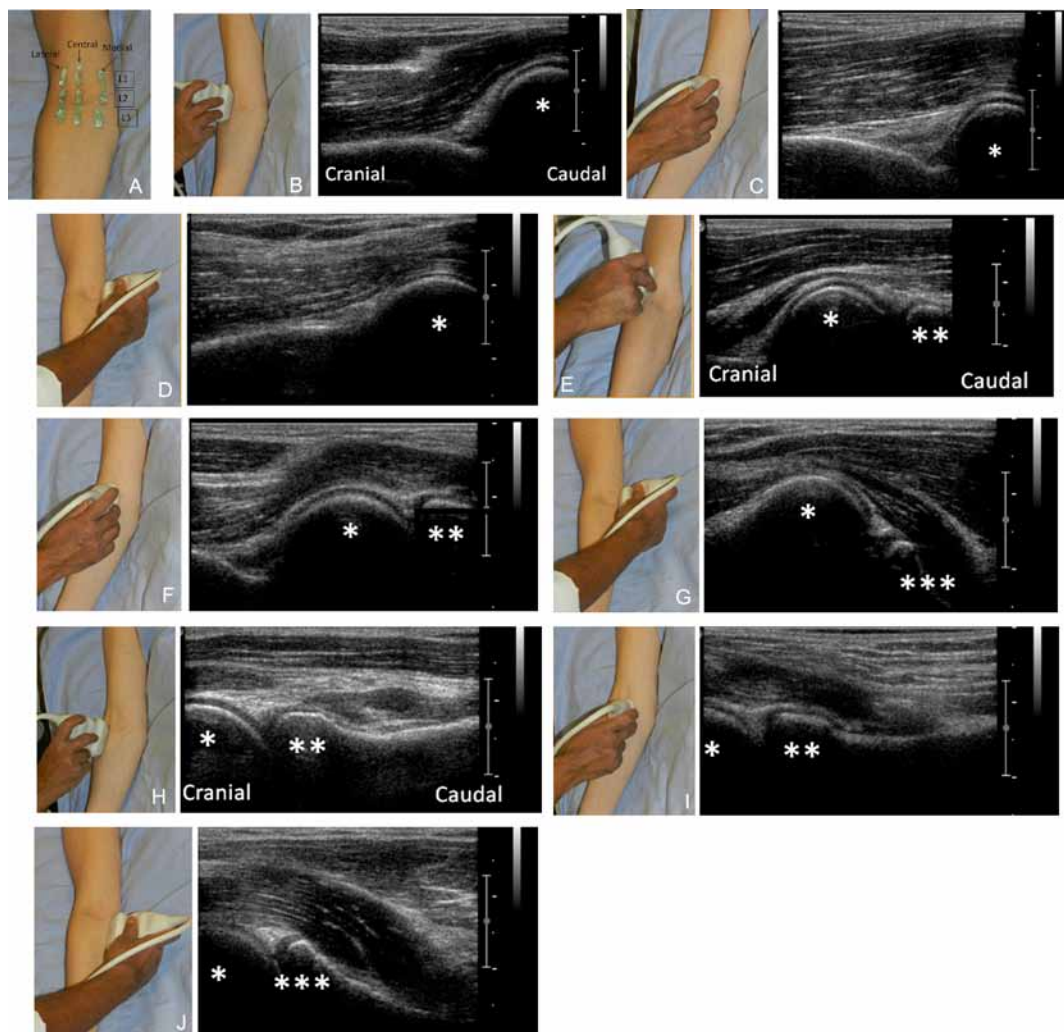


Figure 1: The locations delineated with gel in supine position represent the positions of the transducer for acquisition of sagittal anterior images. The levels shown are L1 SAG, ANT, LAT; L1 SAG, ANT, CEN; L1 SAG, MED LAT; L2 SAG, ANT, LAT; L2 SAG, ANT, CEN; L2 SAG, ANT, MED; and L3 SAG, ANT, LAT; L3 SAG, ANT, CEN; L3 SAG, ANT, MED.

Abbreviations: SAG: Sagittal; ANT: Anterior; MED: Medial; CEN: Central; LAT: Lateral

The transducer positions used for sagittal anterior imaging acquisition of the anterior aspect of the elbow joint at the level L1 are shown. The positions of the transducer placed laterally (B), centrally (C) and medially (D) in relation to the central position of the joint are illustrated with accompanying sonographic images in a healthy volunteer. The distal humeral epiphysis (*) has been marked.

The transducer positions used for sagittal imaging acquisition of the anterior aspect of the elbow joint at the level L2 are shown. The positions of the transducer placed laterally (E), centrally (F) and medially (G) in relation to the central position of the joint are illustrated with accompanying sonographic images in a healthy volunteer. The distal humeral epiphysis (*) and proximal epiphysis of the radius (**) and coronoid process of the ulna (***) have been marked.

The transducer positions used for sagittal imaging acquisition of the anterior aspect of the elbow joint at the level L3 are shown. The positions of the transducer placed laterally (H), centrally (I) and medially (J) in relation to the central position of the joint are illustrated with accompanying sonographic images in a healthy volunteer. The distal humeral epiphysis (*) and proximal epiphysis of the radius (**) and coronoid process of the ulna (***) have been marked.

[subchondral cysts (Figure 6), bone erosions (Figure 6) and cartilage loss (Figure 7)] abnormalities. A prior study [17] reported in detail the expected ultrasound echogenicity and MRI signal intensity for soft tissue and osteochondral abnormalities in hemophilic arthropathy of knees and ankles which is also applicable to the elbow joint.

After several hemarthroses in hemophilic joints, the synovium often appears as a thickened irregular hypoechoic band lying over anechoic hyaline cartilage. Chronologically, the sonographic progression of synovitis occurs with thickening and irregularity of the echogenic synovial line which eventually develops villousities in advanced stages

[8]. In cases of cartilage degeneration, tears may develop in the cartilage, which appears irregular and subchondral cysts may be apparent.

Color Doppler images typically show an increase in the blood supply to the synovium as part of the inflammatory process [6] as shown in Figure 6. With regard to the value of power Doppler ultrasound in the diagnosis of hemophilic synovitis, a prior study [18] that investigated knees, elbows and ankles of children and adults who had history of > 2 lifetime hemarthroses showed that measurements of synovial thickness ($r = 0.70$, $P < 0.0001$) and synovial vascularity ($r = 0.73$, $P < 0.0001$) obtained with power Doppler ultrasound correlated strongly with those obtained with dynamic contrast-enhanced MRI. Nevertheless, to our



Figure 2: The locations delineated with gel in supine position represent the positions of the transducer for acquisition of true lateral (A) and true medial (B) ultrasound images. The levels shown are L1, COR, LAT; L2, COR, LAT; L3, COR, LAT; and L1, COR, MED; L2, COR, MED; L3, COR, MED.

Abbreviations: COR: Coronal; MED: Medial; LAT: Lateral

The transducer positions used for true lateral imaging acquisition of the elbow joint at the levels L1, L2 and L3 are shown. The positions of the transducer placed laterally at the level L1 (C), L2 (D) and L3 (E) in relation to the central position of the joint are illustrated with accompanying sonographic images in a healthy volunteer. The distal humeral epiphysis (*) and proximal epiphysis of the radius (**) have been marked.

The transducer positions used for true medial imaging acquisition of the elbow joint at the levels L1, L2 and L3 are shown. The positions of the transducer placed medially at the level L1 (F), L2 (G) and L3 (H) in relation to the central position of the joint are illustrated with accompanying sonographic images in a healthy volunteer. The distal humeral epiphysis (*) and coronoid process of the ulna (***) have been marked.

knowledge little is known about the value of color and power Doppler ultrasound for staging of blood degradation products in hemophilic joints that suffered prior hemarthroses at different timepoints over the course of the disease. Synovial neovascularization can be assessed with the color Doppler technique using different semi-quantitative [9] or quantitative [18] measurement systems.

Discussion

Previous studies have evaluated sonographic images of joints of hemophilic children with regard to the imaging features [19,20], degree of severity of arthropathy [15] and monitoring of treatment [21,22] and have shown a potential role of ultrasound in the assessment of hemophilic arthropathy, most notably in its early stage. The proposed systematic protocol for imaging of hemophilic elbows adds to previous protocols [9] and is an initial step towards this direction. Melchiorre et al. [9] proposed the use of an interpretation score that classifies hemophilic arthropathy from 0 to 21 points based on a succinct protocol for data acquisition. The current study focuses instead on a more detailed data acquisition protocol.

Table 1 and Figure (1-5) present a standardized protocol for ultrasound imaging of the elbow in hemophilic children. The purpose of the proposed ultrasound imaging acquisition protocol is to facilitate uniform evaluation of hemophilic arthropathy of elbows and to be used with scoring systems for assessment of disease status, progression and effect of therapy. As the experience using this protocol accumulates it

may require further refinement. With specific regard to the elbow joint, which is challenging to be reliably positioned, a detailed description of normal findings on ultrasound is reported elsewhere [8].

Ultrasound may be a useful complementary modality in evaluating the musculoskeletal involvement of joints in children with hemophilia. In contrast to the aforementioned advantages of ultrasound in relation to other imaging modalities, most notably MRI, is the fact that ultrasound is user dependent. Nevertheless, preliminary data from a prior study that evaluated both ultrasound and MRI in hemophilic knees and ankles [23] however showed that the inter-operator reliability of acquisition of gray-scale US images by operators who were blinded and unblinded to corresponding MR images was substantial to excellent.

Some technical approaches used in this study merit clarification. In this study since no pads were used to allow correct joint placement and enable reproducibility of measurements we applied the transducer on the elbow joint in neutral position with the patient in supine or prone position as appropriate.

None of the scanned patients had history of an acute or subacute joint bleed prior to the time of scanning. Therefore, the visualized findings related to chronic arthropathic changes in hemophilic elbows with history of previous hemarthroses. Under other circumstances distinct from those of the current study, such as in the event of an acute bleed prior administration of coagulation factors should have been

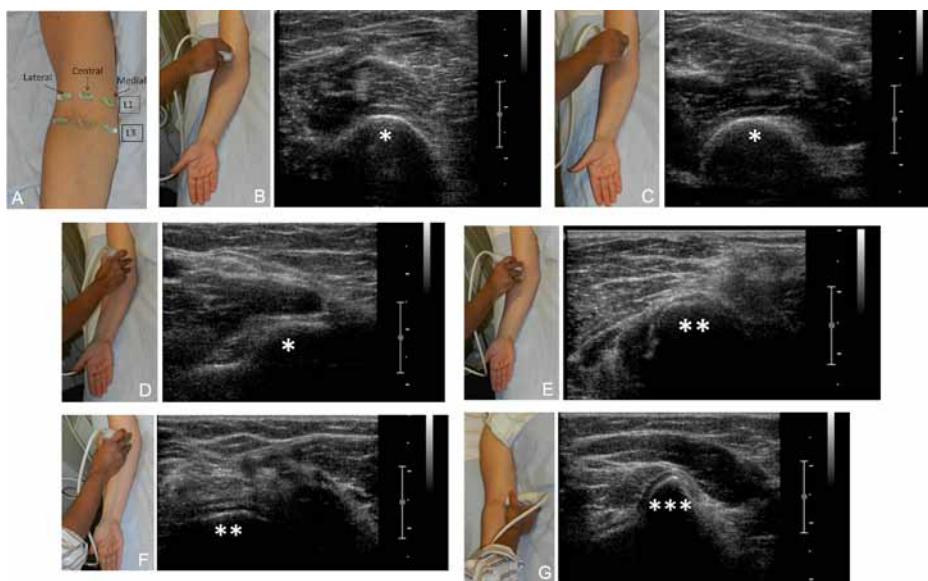


Figure 3: The locations delineated with gel in supine position represent the positions of the transducer for acquisition of axial anterior ultrasound images. The levels shown are L1, AX, ANT, LAT; L1, AX, ANT, CEN; L1, AX, ANT, MED; L2, AX, ANT, LAT; L2, AX, ANT, CEN; L2, AX, ANT, MED; and L3, AX, ANT, LAT; L3, AX, ANT, CEN; L3, AX, ANT, MED.

Abbreviations: ANT: Anterior; AX: Axial; LAT: Lateral; CEN: Central; MED: Medial

The transducer positions used for axial anterior imaging acquisition of the elbow joint at the level L1 are shown. The positions of the transducer placed laterally (B), centrally (C) and medially (D) in relation to the central position of the joint are illustrated with accompanying sonographic images in a healthy volunteer. The distal humeral epiphysis (*) has been marked.

The transducer positions used for axial anterior imaging acquisition of the elbow joint at the level L3 are shown. The positions of the transducer placed laterally (E), centrally (F) and medially (G) in relation to the central position of the joint are illustrated with accompanying sonographic images in a healthy volunteer. The proximal epiphysis of the radius (**) and coronoid process of the ulna (***) have been marked.

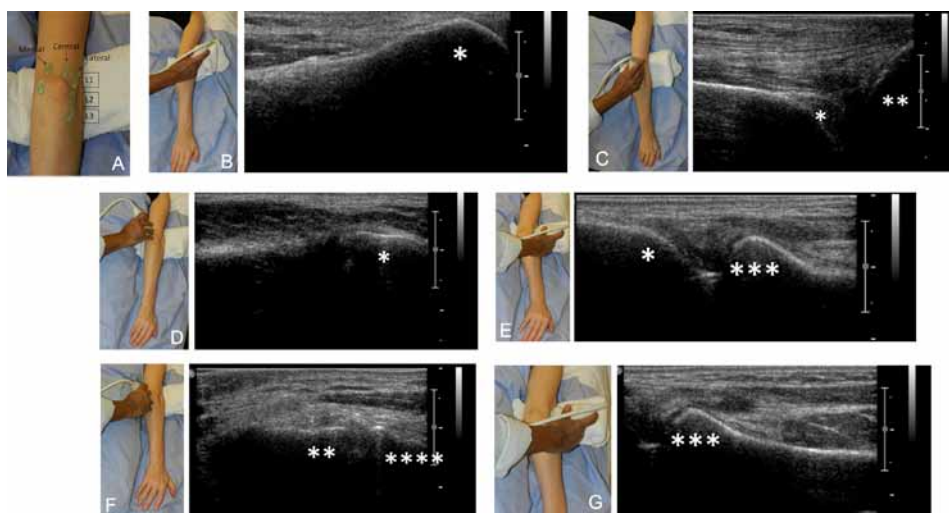


Figure 4: The locations delineated with gel in prone position represent the positions of the transducer for acquisition of sagittal posterior images. The levels shown are L1. SAG, POS, LAT; L1. SAG, POST, CEN; L1 SAG, POST, MED; L2 SAG, POST, LAT; and L3 SAG, POST, LAT.

Abbreviations: SAG: Sagittal; POST: Posterior; LAT: Lateral; CEN: Central; MED: Medial

The transducer positions used for sagittal imaging acquisition of the posterior aspect of the elbow joint at the level L1 are shown. The positions of the transducer placed laterally (B), centrally (C) and medially (D) in relation to the central position of the joint are illustrated with accompanying sonographic images in a healthy volunteer. The distal humerus (*) and ulnar olecranon (**) have been marked.

The transducer positions used for sagittal imaging acquisition of the posterior aspect of the elbow joint at the level L2 are shown. The positions of the transducer placed laterally (E), and medially (F) in relation to the central position of the joint are illustrated with accompanying sonographic images in a healthy volunteer. The humeral lateral (*) and medial (**) epicondyles as well as radial head (***) and proximal ulna (****) have been marked.

The transducer position used for sagittal imaging acquisition of the posterior aspect of the elbow joint at the level L3 is shown. The position of the transducer placed laterally (G) in relation to the central position of the joint is illustrated with accompanying sonographic images in a healthy volunteer. The radial head (***) has been marked.

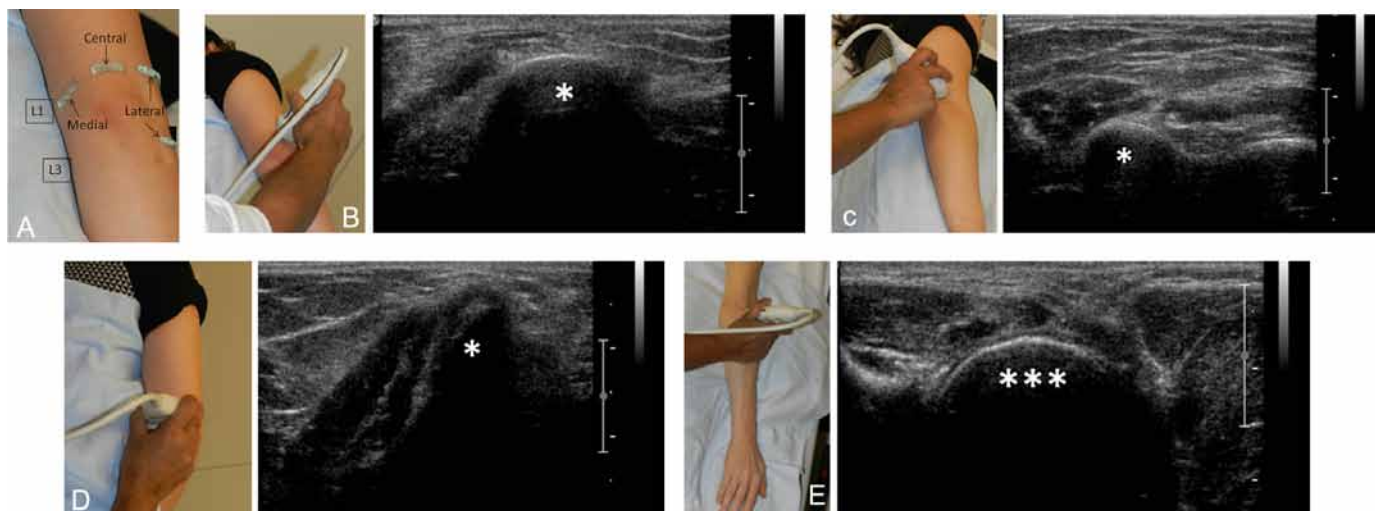


Figure 5: The locations delineated with gel in supine position represent the positions of the transducer for acquisition of axial posterior ultrasound images. The levels shown are L1, AX, POST, LAT; L1, AX, POST, CEN; L1, AX, POST, MED; L3, AX, POST, LAT.

Abbreviations: POST: Posterior; AX: Axial; LAT: Lateral; CEN: Central; MED: Medial

The transducer positions used for axial posterior imaging acquisition of the elbow joint at the level L1 are shown. The positions of the transducer placed laterally (B), centrally (C) and medially (D) in relation to the central position of the joint are illustrated with accompanying sonographic images in a healthy volunteer. The distal humerus (*) has been marked.

The transducer position used for axial posterior imaging acquisition of the elbow joint at the level L3 is shown. The positions of the transducer placed laterally (E) in relation to the central position of the joint is illustrated with accompanying sonographic images in a healthy volunteer. The radial head (***) has been marked.

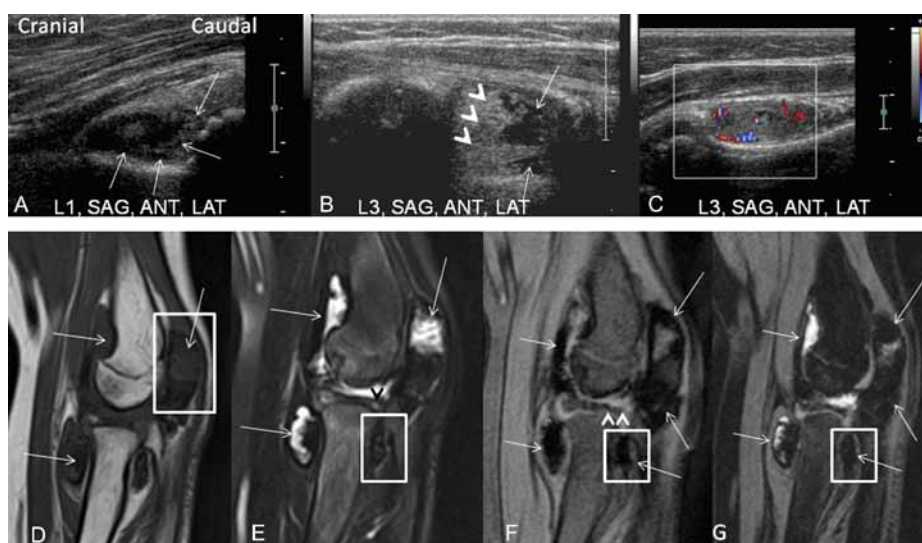


Figure 6: Ultrasound and corresponding MR images of the left elbow of an 11-year old hemophilic boy with history of >5 previous hemarthroses in the study joint, moderate radiographic joint changes (Petterson score, 5, not shown) and Hemophilia Joint Health Score (HJHS) of 6.

Ultrasound: SOFT TISSUES: Gray-scale (A, B) and color Doppler (C) ultrasound images of this elbow demonstrate the large joint effusion (arrow, A, L1 SAG, ANT, LAT level) along with speckles of hemosiderin deposition within the synovium anterior to the distal humeral meta-epiphysis (small arrows, black foci within synovium, A [L1 SAG, ANT, LAT level]) and anterior to the proximal metaphysis of the radius (small arrows, black foci within synovium, F [L3 SAG, ANT, LAT level]). Color Doppler ultrasound reveals moderate synovial hyperemia (C, L3 SAG, ANT, LAT level) anterior to the proximal metaphysis of the radius.

MRI: SOFT TISSUES: Corresponding sagittal turbo spin-echo T1-weighted (D), T2-weighted fast spin-echo (E), Multi-Echo Data Image Combination [MEDIC] (F) and 3D water excitation Double Echo Steady State [DESS] (G) MR images of this elbow show a large joint effusion (arrows, D, E), and extensive hemosiderin deposition and synovial hypertrophy (arrows, F, G).

MRI: OSTEOCHONDRAL TISSUES: In addition to the aforementioned soft tissue changes, subchondral cysts are identified within the radial head (arrowhead, E). Articular surface irregularities are seen along the capitellum and radial head suggestive of bone erosions (arrowheads, F).

Please find within the boxes with white lining on MR images the regions-of-interest that were assessed with ultrasound on corresponding images: A (ultrasound) and D (MRI), L1 SAG, ANT, LAT level; B, C (ultrasound) and E, F, G (MRI), L3 SAG, ANT, LAT level.

Abbreviations: L1, SAG, ANT, LAT, L1 sagittal anterior lateral level; L3, SAG, ANT, LAT, L3 sagittal anterior lateral level.

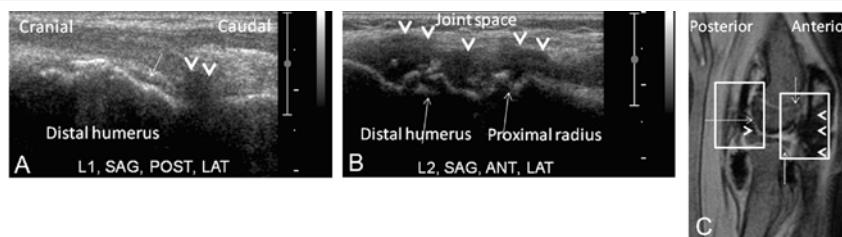


Figure 7: Gray-scale ultrasound images (A, B) of the left elbow of the 11-year old hemophilic boy of Fig. 6 are compared with the corresponding gradient-echo [Multi-Echo Data Image Combination, MEDIC] MR image (C). The boxes with white lining on the MR image (A) show the regions-of-interest of the ultrasound images.

Ultrasound: OSTEOCHONDRAL TISSUES: Caption A obtained at the posterior aspect of the distal humeral meta-epiphysis (L1 POST, SAG, LAT level) shows loss of half or more of the total volume of joint cartilage in at least one bone, the humerus (short arrow), along with hemosiderin deposition at the joint space (arrowheads).

MR: OSTEOCHONDRAL TISSUES: The arrow within the posterior white line box demonstrates cartilage loss and the arrowhead within this box demonstrates joint space hemosiderin deposition on the corresponding MR image (C).

Ultrasound: SOFT TISSUES: Caption B obtained at the anterior aspect of the joint space (L2 SAG, ANT, LAT level) demonstrates large synovial hypertrophy (lighter gray) and hemosiderin deposition (darker gray) [arrowheads] along the anterior aspect of the distal humeral meta-epiphysis, joint space and anterior aspect of the proximal radial meta-epiphysis. The gross osteochondral irregularities (arrows) represent the growth plates of the distal humerus and proximal radius.

MR: SOFT TISSUES: The arrows within the anterior white line box demonstrate the growth plates of the distal humerus and proximal radius. The arrowheads within this box represent hemosiderin deposition overlying and obscuring the adjacent synovial hypertrophy on the corresponding MR image (C).

Abbreviations: L1, SAG, POST, LAT, L1 sagittal posterior lateral level; L2, SAG, ANT, LAT, L2 sagittal anterior lateral level.

View	Anatomic Landmarks	Tissue Visualization
Anterior – patient supine (Figure 1A, Figure B-D)	L1, SAG, ANT, MED; L1, SAG, ANT, CEN; L1, SAG, ANT, LAT	Cartilage, soft tissues
Anterior – patient supine (Figure 1A, Figure E-G)	L2, SAG, ANT, MED; L2, SAG, ANT, CEN; L2, SAG, ANT, LAT	Cartilage, soft tissues
Anterior – patient supine (Figure 1A, Figure H-J)	L3, SAG, ANT, MED; L3, SAG, ANT, CEN; L3, SAG, ANT, LAT	Cartilage, soft tissues
True lateral (Figure 2A, Figure C-E)	L1, COR, LAT; L2, COR, LAT; L3, COR, LAT	Cartilage, soft tissues
True medial (Figure 2B, Figure F-H)	L1, COR, MED; L2, COR, MED; L3, COR, MED	Cartilage, soft tissues
Anterior – patient supine (Figure 3A, Figure B-D)	L1, AX, ANT, MED; L1, AX, ANT, CEN; L1, AX, ANT, LAT	Cartilage, soft tissues
Anterior – patient supine (Figure 3A, Figure E-G)	L3, AX, ANT, MED; L3, AX, ANT, CEN; L3, AX, ANT, LAT	Cartilage, soft tissues
Posterior – patient prone (Figure 4A, Figure B-D)	L1, SAG, POST, MED*; L1, SAG, POST, CEN*; L1, SAG, POST, LAT*	Cartilage, bursa (olecraneal)
Posterior – patient prone (Figure 4A, Figure E, F)	L2, SAG, POST, MED*; L2, SAG, POST, LAT*	Cartilage, soft tissues
Posterior – patient prone (Figure 4A, Figure G)	L3, SAG, POST, LAT	Cartilage, soft tissues
Posterior – patient prone (Figure 5A, Figure B-D)	L1, AX, POST, MED*; L1, AX, POST, CEN*; L1, AX, POST, LAT*	Cartilage, bursa (olecraneal)
Posterior – patient prone (Figure 5A, Figure E)	L3, AX, POST, LAT	Cartilage, soft tissues

Abbreviations: ANT: Anterior; POST: Posterior; SAG: Sagittal; AX: Axial; MED: Medial; CEN: Central; LAT: Lateral; COR: Coronal
*Additional Doppler required: L1, above the joint line; L2, at the joint line; L3, below the joint line.

Table 1: Transducer position in the sagittal, coronal and axial planes for ultrasound scanning of the elbows. Standard anatomic descriptions for the level of transducer position: L1 for proximal articular surface (above the elbow joint), L2 for joint space and L3 for distal articular surface (below the elbow joint).

required prior to the ultrasound scan to reduce local pain and avoid further hemarthrosis.

The proposed ultrasound protocol does not include posterior sagittal or axial views through the medial aspect of the proximal ulna (Table) because the presence of the ulnar olecranon precludes the need for assessment of cartilage at the L3 level.

Although previous studies [9] have recommended 90° of arm flexion and the forearm planted perpendicular to the surface of the examination table to study the posterior elbow recess, we felt that the neutral position (or the position closest to that) may enable higher reproducibility of results in patients with upper extremity deformity and facilitate the cooperation of patients with arthropathy. Although the use of neutral position for ultrasound scanning enables assessment

of the posterior, lateral and medial aspects of the posterior distal humeral region, measurement variabilities are expected in hemophilic patients with joint contractures. Further investigation is needed in the future to assess the inter- and intrareader reliability of soft tissue and osteochondral abnormalities using specific ultrasound [23] scoring systems and to validate/refine the proposed protocol.

Limitations of this protocol development study include the small sample size of patients and the inability to investigate the impact of elbow joint contractures on the ultrasound scanning feasibility. Nevertheless, the purpose of this study was to systematically define regions-of-interest and sonographic planes in the elbow and to assure that soft tissue (joint effusion/hemarthrosis, synovial hypertrophy, hemosiderin deposition) and osteochondral (subchondral cysts, bone erosions and cartilage loss) abnormalities can be depicted by the proposed ultrasound protocol in blood-induced arthropathy. For this purpose the main inclusion criteria for the study were to be a male within the expected age range of the study and to present with a blood-induced arthropathy that affected one of the elbows. A study with similar characteristics of the patient population (except for the diagnosis of von Willebrand disease and for the presence of arthropathy in a different joint, one knee or ankle) was conducted by our group on a systematic ultrasound protocol for assessment of hemophilic knees and ankles [17].

Three major bursae are located at the elbow joint. First is the subcutaneous olecranon bursa, found in the connective tissue over the olecranon; second is the intratendinous olecranon bursa found in the triceps brachii tendon; and third is the subtendinous olecranon bursa, which reduces the friction between the triceps tendon and the olecranon proximal to its insertion on the olecranon [24]. The proposed protocol is expected to visualize the superficial components of the olecranon bursae. The feasibility of assessment of deeper components of this bursa will depend on the depth of the field-of-view on a given ultrasound image. This is an inherent technical limitation of the sonographic imaging modality.

In conclusion, systematization of imaging acquisition protocols is essential for comparison of results of clinical trials in the future. Although the proposed technique can be reliable in clinical and research settings when applied by experienced hands [23], hemophilia treatment centres must develop capacity to train expert physicians / sonographers specialized in ultrasound; provide sufficient scanning time for a detailed or limited examination as per clinical indication and adjust the technique according to the availability of transducers and scanner generation capability. The proposed protocol for ultrasound data acquisition in hemophilic elbows adds to the reservoir of knowledge in the field. Correlation with corresponding MR images improves our understanding of limitations of the ultrasound technique tailoring its clinical applications. To avoid a multiplicity of available protocols for imaging assessment of hemophilic joints future consensus meetings are required to establish a single systematic protocol which can be adjusted to different levels of complexity according to the clinical setting and imaging equipment capability of the hemophilia centres. The proposed ultrasound protocol for assessment of elbows should serve the aforementioned purpose requiring equipments already available in most hemophilia centres in the world. This protocol should however be optimized to address different clinical questions and health care system realities in the near future. Of utmost importance is to note that further validation of ultrasonography as an outcome measure to guide response to treatment and to enable follow-up of children under prophylaxis is required.

Acknowledgement

Dr. Frederico Xavier was a trainee (fellow) in the pediatric thrombosis and hemostasis program, Division of Hematology/Oncology, Hospital for Sick Children, Toronto, Canada during the period 2010 – 2011. Funding support for Dr. Xavier's fellowship was provided by Pfizer, Canada.

Dr. Ningning Zhan received a World Federation of Hemophilia 6-month fellowship award and a Bayer Canada grant during part of the conduct of this study at The Hospital for Sick Children, Toronto, Canada in 2010.

References

1. Baunin C, Railhac JJ, Younes I, Gaubert J, du Boullay C, et al. (1991) MR imaging in hemophilic arthropathy. *Eur J Pediatr Surg* 1: 358-363.
2. Hilgartner MW (2002) Current treatment of hemophilic arthropathy. *Curr Opin Pediatr* 14: 46-49.
3. Rand T, Trattnig S, Male C, Heinz-Peer G, Imhof H, et al. (1999) Magnetic resonance imaging in hemophilic children: value of gradient echo and contrast-enhanced imaging. *Magn Reson Imaging* 17: 199-205.
4. Resnick D (2002) *Diagnosis of Bone and Joint Disorders*. Philadelphia: Saunders.
5. Manco-Johnson MJ, Pettersson H, Petrini P, Babyn PS, Bergstrom BM, et al. (2004) Physical therapy and imaging outcome measures in a haemophilia population treated with factor prophylaxis: current status and future directions. *Haemophilia* 10: 88-93.
6. Rodriguez-Merchan EC, Jimenez-Yuste V, Aznar JA, Hedner U, Knobe K, et al. (2011) Joint protection in haemophilia. *Haemophilia* 17: 1-23.
7. Doria AS, Kraft J, Babyn P, Demers C, Israelis S, et al. (2011) Magnetic resonance imaging and joint outcomes in boys with severe hemophilia A treated with tailored primary prophylaxis in a multicentre clinical trial in Canada. *Pediatr Radiol* 41: 291-292.
8. Querol F, Rodriguez-Merchan EC (2011) The role of ultrasonography in the diagnosis of the musculo-skeletal problems of haemophilia. *Haemophilia*.
9. Melchiorre D, Linari S, Innocenti M, Biscoglio I, Toigo M, et al. (2011) Ultrasound detects joint damage and bleeding in haemophilic arthropathy: a proposal of a score. *Haemophilia* 17: 112-117.
10. Beals RK (1976) The normal carrying angle of the elbow. A radiographic study of 422 patients. *Clin Orthop Relat Res*: 194-196.
11. Moore KL, Dalley AF (2009) *Clinically Oriented Anatomy*. Lippincott Williams & Wilkins.
12. Feldman BM, Funk SM, Bergstrom BM, Zourikian N, Hilliard P, et al. (2011) Validation of a new pediatric joint scoring system from the International Hemophilia Prophylaxis Study Group: validity of the hemophilia joint health score. *Arthritis Care Res (Hoboken)* 63: 223-230.
13. Keshava S, Gibikote S, Mohanta A, Doria AS (2009) Refinement of a sonographic protocol for assessment of haemophilic arthropathy. *Haemophilia* 15: 1168-1171.
14. Pettersson H, Ahlberg A, Nilsson IM (1980) A radiologic classification of hemophilic arthropathy. *Clin Orthop Relat Res* : 153-159.
15. Klukowska A, Czyrny Z, Laguna P, Brzewski M, Serafin-Krol MA, et al. (2001) Correlation between clinical, radiological and ultrasonographical image of knee joints in children with haemophilia. *Haemophilia* 7: 286-292.
16. Martin-Hervas C, Rodriguez-Merchan EC (2011) Imaging of the hemophilic joint. In: Rodriguez-Merchan EC, Valentino LA, eds. *Current and Future Issues in Hemophilia*. London: Wiley-Blackwell: 121-26.
17. Zukotynski K, Jarrin J, Babyn PS, Carcao M, Pazmino-Canizares J, et al. (2007) Sonography for assessment of haemophilic arthropathy in children: a systematic protocol. *Haemophilia* 13: 293-304.
18. Acharya SS, Schloss R, Dyke JP, Mintz DN, Christos P, et al. (2008) Power Doppler sonography in the diagnosis of hemophilic synovitis—a promising tool. *J Thromb Haemost* 6: 2055-2061.
19. Hermann G, Gilbert MS, Abdelwahab IF (1992) Hemophilia: evaluation of musculoskeletal involvement with CT, sonography, and MR imaging. *AJR Am J Roentgenol* 158: 119-123.
20. Merchan EC, De Orbe A, Gago J (1992) Ultrasound in the diagnosis of the early stages of hemophilic arthropathy of the knee. *Acta Orthop Belg* 58: 122-125.

-
21. Wallny T, Brackmann HH, Semper H, Schumpe G, Effenberger W, et al. (2000) Intra-articular hyaluronic acid in the treatment of haemophilic arthropathy of the knee. Clinical, radiological and sonographical assessment. *Haemophilia* 6: 566-570.
22. Aznar JA, Abad-Franch L, Perez-Alenda S, Haya S, Cid AR, et al. (2011) Ultrasonography in the monitoring of management of haemarthrosis. *Haemophilia* 17: 826-828.
23. Doria AS, Keshava S, Mohanta A, Jarrin J, Man C, et al. (2010) Reliability of Blinded and Unblinded Acquisition and Interpretation of Ultrasound for Assessment of Hemophilic Knees and Ankles, Proceedings of the XXIX International Congress of the World Federation of Hemophilia. Buenos Aires, Argentina.
24. Kishner S (2011) Elbow Joint Anatomy.

This article was originally published in a special issue, **Musculo Skeletal Examination** handled by Editor(s). Dr. Olwyn Westwood, Barts & The London School of Medicine and Dentistry, UK